

Supplementary Information

New insights into the mechanism of activation of atom transfer radical polymerization by Cu(I) complexes

Patrizia De Paoli, Abdirisak A. Isse,* Nicola Bortolamei and Armando Gennaro

Department of Chemical Sciences, University of Padova, via Marzolo 1, 35131 Padova, Italy
abdirisak.ahmedisse@unipd.it

Table of contents

1. Experimental section	S2
2. Distribution diagrams of Cu–Me ₆ TREN–X [−] systems	S3
3. Voltammetric behavior of the ternary Cu–Me ₆ TREN–X [−] system	S4
4. Chronoamperometric determination of activation rate constants	S6
5. Determination of activation rate constants in the presence of halide ions	S8

1. Experimental section

Chemicals. Acetonitrile (Carlo Erba, RS) was distilled over CaH₂ and stored under argon atmosphere. Tetraethylammonium tetrafluoroborate (Et₄NBF₄, Alfa Aesar, 99%) was recrystallized from ethanol and dried in a vacuum oven at 70 °C for 48 h. Tetraethylammonium chloride (Aldrich, 98%) and tetraethylammonium bromide (Aldrich, 99%) were recrystallized from dichloromethane-acetone-hexane (2:2:1) and ethanol-diethyl ether, respectively, and were dried in a vacuum oven at 70 °C. In the latter case, recrystallization was performed by dissolving the salt in ethanol and then adding diethyl ether until crystallization starts. Tris(2-dimethylaminoethyl)amine (Me₆TREN) was prepared according to a published procedure,¹ by methylation of tris(2-aminoethyl)amine (TREN) in a mixture of formaldehyde and formic acid and was purified by vacuum distillation. Copper(II) trifluoromethanesulfonate (Aldrich, 98%), tetrakis(acetonitrile)copper(I) tetrafluoroborate (Aldrich, 97%), benzyl chloride (Fluka, 99%), chloroacetonitrile (Fluka, 99%), ethyl bromoacetate (Aldrich, 98%), allyl bromide (Aldrich, 97%) and 2,2,6,6-tetramethyl-1-piperidinyloxy (TEMPO, Aldrich, 98%) were used without further purification.

Linear sweep voltammetry. Electrochemical measurements were carried out on a computer-controlled Autolab PGSTAT30 potentiostat (Eco-Chimie, Utrecht, Netherlands). All experiments were carried out in a three-electrode airtight cell system under argon atmosphere, using a rotating disk electrode (RDE, Autolab, Eco-Chimie) with a glassy carbon tip (GC) disc (3 mm diameter, Metrohm) as a working electrode, and a Pt ring as a counter-electrode. The reference electrode was a Ag|AgI|I⁻ electrode built as described previously.² The potential of this reference electrode was always measured versus the ferrocenium/ferrocene couple ($E^{\circ}_{\text{Fc}^+/\text{Fc}} = 0.391 \text{ V vs SCE in MeCN}$), which was used as an internal standard. This has allowed conversion of the potentials to the aqueous saturated calomel electrode (SCE) scale to which all potentials reported in the paper are referenced. The cell had a double wall jacket through which water from a thermostated bath (Thermo Scientific, HAAKE SC100) was circulated. All experiments were carried out at 25 ± 0.1 °C, except those performed to study the temperature effect. Prior to each experiment the working electrode surface was cleaned by polishing with a 0.25- μm diamond paste, followed by ultrasonic rinsing in ethanol for 5 minutes.

Chronoamperometry. Kinetic experiments were carried out using the system described above. Prior to the solvent introduction, the cell with all electrodes was carefully fluxed with Ar at least for 30 min to avoid the presence of oxygen in the reaction environment. Cu^IL⁺ (L = Me₆TREN) was

prepared in-situ by mixing stoichiometric amounts of $[\text{Cu}^{\text{I}}(\text{MeCN})_4]\text{BF}_4$ and Me_6TREN . When the effect of X^- was of interest the required amount of the halide was added as $(\text{C}_2\text{H}_5)_4\text{NCl}$ or $(\text{C}_2\text{H}_5)_4\text{NBr}$. A typical concentration of the complex was 0.5 mM, whereas C_{X^-} was varied from 0 up to 6 mM to investigate the effect of the halide ions on the activation kinetics. TEMPO was always introduced in a large excess with respect to the catalyst ($[\text{TEMPO}]/[\text{Cu}^{\text{I}}\text{L}^+] \geq 10$) in order to ensure the total capture of the alkyl radicals.

The choice of the applied step potential E_f was based on the voltammetric response of the system before addition of RX. The potential was stepped from an initial value before the oxidation wave of $\text{Cu}^{\text{I}}\text{L}^+$ to a value in the plateau region, about 200 mV after the wave. When the reaction was monitored by following the increase of the concentration of $\text{XCu}^{\text{II}}\text{L}^+$, the initial potential was chosen somewhere before the reduction wave of the Cu^{II} complex, whereas the final potential was set at a value in the plateau region of the reduction wave.

2. Distribution diagrams of Cu–Me₆TREN–X[−] systems

Speciations of Cu^{II} and Cu^{I} in the presence of Me_6TREN and halide ions were calculated with Hyperquad 2009³ by using published data for the stability constants of various Cu^{II} and Cu^{I} complexes.⁴ All calculations were carried out with $C_{\text{Cu}}^0 = C_{\text{L}}^0 = 5 \times 10^{-4}$ M and variable $C_{\text{X}^-}^0$ (from

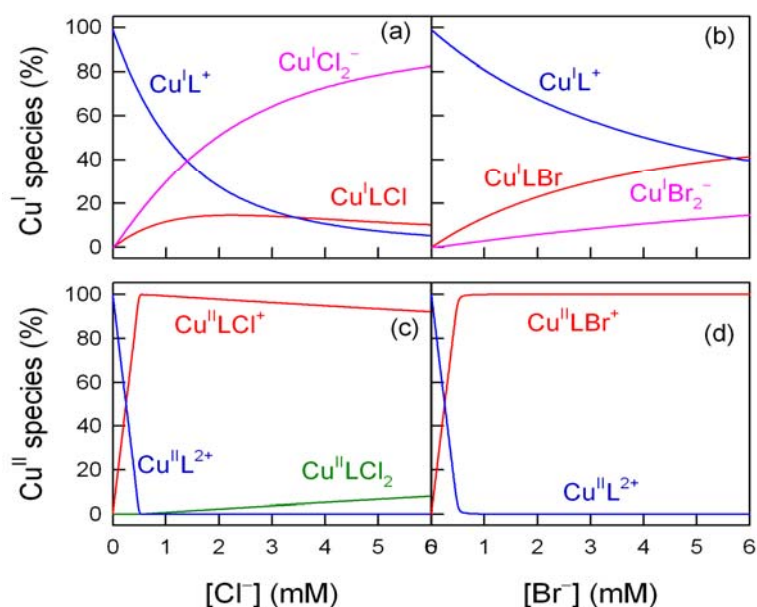


Figure S1. Distribution diagrams of ternary Cu–L–X[−] systems in MeCN + 0.1 M Et₄NBF₄ at 25 °C, $C_{\text{Cu}}^0 = C_{\text{L}}^0 = 5 \times 10^{-4}$ M. a) $\text{Cu}^{\text{I}}\text{L}^+ - \text{L} - \text{Cl}^-$, b) $\text{Cu}^{\text{I}}\text{L}^+ - \text{L} - \text{Br}^-$, c) $\text{Cu}^{\text{II}}\text{L}^{2+} - \text{L} - \text{Cl}^-$, d) $\text{Cu}^{\text{II}}\text{L}^{2+} - \text{L} - \text{Br}^-$. Species representing less than 5% of the total Cu were omitted.

0 to 6×10^{-3} M). The distribution diagrams (Fig. S1) were plotted to show the percentage of each Cu^{II} or Cu^{I} species as a function of the total concentration of X^- .

3. Voltammetric behavior of the ternary $\text{Cu}-\text{Me}_6\text{TREN}-\text{X}^-$ system

Linear sweep voltammetry of *in-situ* prepared $\text{Cu}^{\text{I}}\text{L}^+$ ($\text{L} = \text{Me}_6\text{TREN}$) in $\text{MeCN} + 0.1 \text{ M Et}_4\text{NBF}_4$ at a glassy carbon RDE shows a well defined anodic wave with $E_{1/2} = -0.11 \text{ V vs SCE}$ corresponding to the monoelectronic oxidation of Cu^{I} to Cu^{II} (Fig. S2, curve a). This wave is attributed to the oxidation of $\text{Cu}^{\text{I}}\text{Me}_6\text{TREN}^+$ because this is the only Cu^{I} species present in solution as long as $[\text{Cu}^{\text{I}}] = [\text{L}]$.⁴ The pattern changes in the presence of chloride ions (Fig. S2, curves b-e), showing a new wave at less positive potentials ($E_{1/2} = -0.43 \text{ V vs SCE}$), which is assigned to the oxidation of the ternary complex $\text{ClCu}^{\text{I}}\text{L}$. A third small wave due to the oxidation of $\text{Cu}^{\text{I}}\text{Cl}_2^-$ to $\text{Cu}^{\text{II}}\text{Cl}_2$ could be observed at much higher potentials (not shown in the figure), especially at high Cl^- concentrations. It is to be noted that the oxidation wave of $\text{ClCu}^{\text{I}}\text{L}$ is always much higher than that of $\text{Cu}^{\text{I}}\text{L}^+$, which apparently indicates that $\text{ClCu}^{\text{I}}\text{L}$ is the major species present in solution. This observation is clearly at variance with the results of the speciation calculations for the ternary $\text{Cu}^+-\text{L}-\text{Cl}^-$ system reported in Fig. S1, which show that the amount $\text{ClCu}^{\text{I}}\text{L}$ formed at equilibrium never exceeds 15% (Fig. S1a). This apparent contradiction can be easily explained by noting that the oxidation wave at -0.43 V vs SCE involves not only the quantity of $\text{ClCu}^{\text{I}}\text{L}$ present at

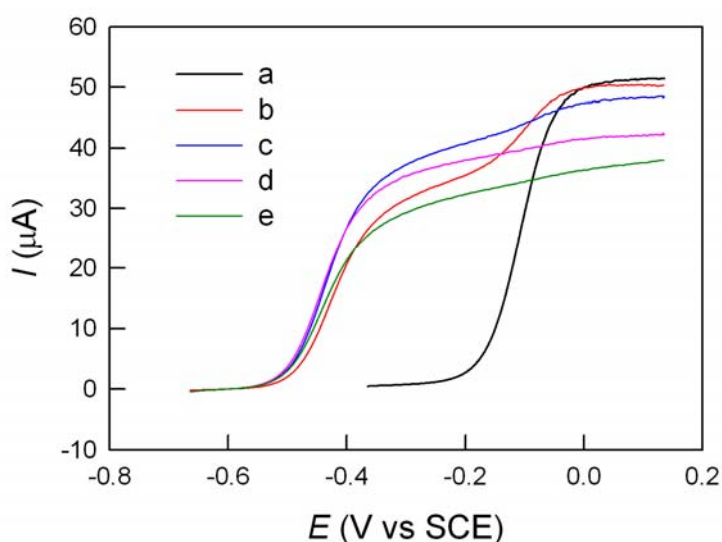


Figure S2. Linear sweep voltammetry of $0.50 \text{ mM } [\text{Cu}^{\text{I}}(\text{MeCN})_4]\text{BF}_4 + 0.50 \text{ mM Me}_6\text{TREN}$ in the absence (a) and presence of (b) 0.66 mM Cl^- , (c) 1.29 mM Cl^- , (d) 2.79 mM Cl^- , (e) 5.44 mM Cl^- , recorded at $\nu = 0.005 \text{ V/s}$ and $\omega = 2500 \text{ rpm}$ in $\text{MeCN} + 0.1 \text{ M Et}_4\text{NBF}_4$ at $25 \text{ }^\circ\text{C}$.

equilibrium but also $\text{ClCu}^{\text{I}}\text{L}$ forming from $\text{Cu}^{\text{I}}\text{L}^+$ and $\text{Cu}^{\text{I}}\text{Cl}_2^-$ during the oxidation process as the speciation equilibria are perturbed near the electrode. In other words, as $\text{ClCu}^{\text{I}}\text{L}$ is consumed at the electrode, the set of equilibrium reactions for the speciation of Cu^{I} respond to the decrease of $\text{ClCu}^{\text{I}}\text{L}$ concentration in the diffusion layer by continuously re-adjusting the equilibrium concentrations. The effect of all these dynamic equilibria is to produce an oxidation wave representing a $[\text{ClCu}^{\text{I}}\text{L}]$ value higher than the bulk equilibrium one.

Addition of bromides to a solution of $\text{Cu}^{\text{I}}\text{L}^+$ causes similar modifications to the voltammetric pattern of the complex (Fig. S3); a new wave appears at more negative potentials ($E_{1/2} = -0.35$ V vs SCE), while that of $\text{Cu}^{\text{I}}\text{L}^+$ decreases and eventually disappears. Also in this case, the new wave does not simply represent the quantity of $\text{BrCu}^{\text{I}}\text{L}$ present in the bulk solution; it contains a contribution from the dynamic equilibria involving all Cu^{I} species present in solution.

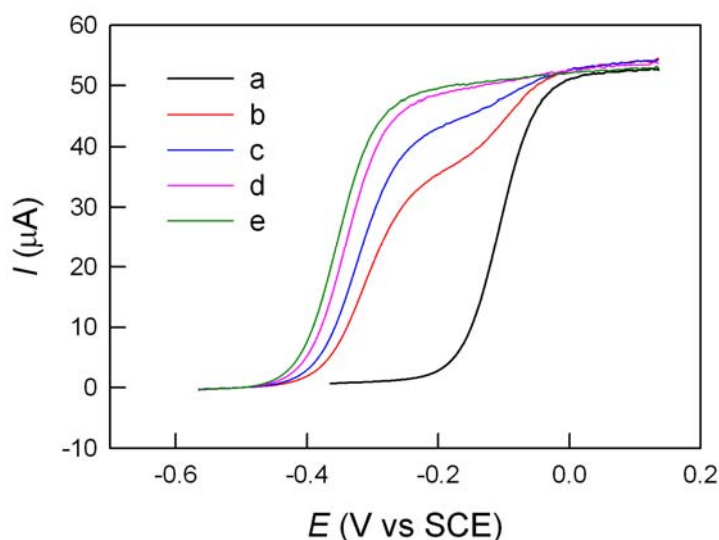


Figure S3. Linear sweep voltammetry of 0.50 mM $[\text{Cu}^{\text{I}}(\text{MeCN})_4]\text{BF}_4$ + 0.50 mM Me_6TREN in the absence (a) and presence of (b) 0.60 mM Br^- , (c) 1.09 mM Br^- , (d) 2.73 mM Br^- , (e) 5.68 mM Br^- , recorded at $\nu = 0.005$ V/s and $\omega = 2500$ rpm in $\text{MeCN} + 0.1$ M Et_4NBF_4 at 25 °C.

In the case of Cu^{II} the effect of $[\text{X}^-]$ on the distribution is much less complicated than that of Cu^{I} as shown in Fig. S1 (c and d). The predominant species under a wide range of $[\text{X}^-]$ values is the mixed complex $\text{XCu}^{\text{II}}\text{L}^+$. In particular, when $[\text{X}^-]/[\text{Cu}^{\text{II}}\text{L}] = 1$, $\text{XCu}^{\text{II}}\text{L}$ is the only species present in solution. Figure S4 illustrates the effect of chloride ions on the voltammetric response of $\text{Cu}^{\text{II}}\text{L}^{2+}$. Addition of Cl^- causes disappearance of the reduction wave of $\text{Cu}^{\text{II}}\text{L}^{2+}$, being substituted by a new wave with $E_{1/2} = -0.43$ V vs SCE due to the reduction of $\text{ClCu}^{\text{II}}\text{L}^+$. It is interesting to note that a

single wave with almost a constant limiting current is observed even in the presence of excess Cl^- . A similar behavior has been observed also for bromide ions.

The above described voltammetric investigations on the ternary systems involving X^- , L and Cu^{I} or Cu^{II} , show that a simple voltammetric response is obtained with Cu^{II} complexes. Conversely, the $\text{Cu}^{\text{I}}\text{-L-X}^-$ system shows a more complicated voltammetric behavior. In particular, the oxidation wave observed for $\text{XCu}^{\text{I}}\text{L}$ cannot be easily related to the real equilibrium concentration of the complex present in the bulk medium. This represents a big problem for the kinetic analysis if one desires to monitor the activation reaction by following the decay rate of Cu^{I} . In contrast, there are no problems with Cu^{II} ; only one species is formed and consequently a single wave, which is proportional to its concentration, is observed. The reaction kinetics can be monitored by following the increase of $\text{XCu}^{\text{II}}\text{L}^+$. Therefore, the kinetics of all experiments related to the effect of X^- on the reaction rate has been studied by using the reduction wave of $\text{XCu}^{\text{II}}\text{L}^+$ as a redox probe.

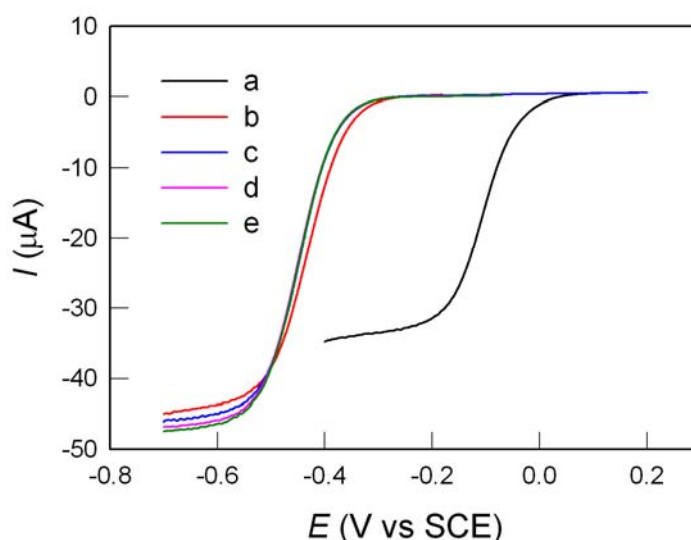


Figure S4. Linear sweep voltammetry of 0.50 mM $\text{Cu}^{\text{II}}(\text{CF}_3\text{SO}_3)_2$ + 0.50 mM Me_6TREN in the absence (a) and presence of (b) 0.54 mM Cl^- , (c) 1.13 mM Cl^- , (d) 2.74 mM Cl^- , (e) 5.18 mM Cl^- , recorded at $\nu = 0.005$ V/s and $\omega = 2500$ rpm in $\text{MeCN} + 0.1$ M Et_4NBF_4 at 25 °C.

4. Chronoamperometric determination of activation rate constants

The voltammetric responses shown above pointed out that when the species present in solution is $\text{Cu}^{\text{I}}\text{L}^+$, the reaction with RX can be monitored by following either the disappearance of the oxidation current of $\text{Cu}^{\text{I}}\text{L}^+$ or the increase of the reduction current of $\text{XCu}^{\text{II}}\text{L}^+$. In general, the kinetic investigations of the activation of RX by $\text{Cu}^{\text{I}}\text{L}^+$ without added X^- were performed by following the disappearance of $\text{Cu}^{\text{I}}\text{L}^+$ on a rotating disc electrode (RDE) at $\omega = 2500$ rpm. The

chronoamperometric experiment was started with a solution of $\text{Cu}^{\text{I}}\text{L}^+$ by stepping the RDE potential from -0.3 V to 0.1 V vs SCE. The current rises from zero to a limiting value corresponding to the diffusion-controlled oxidation of $\text{Cu}^{\text{I}}\text{L}^+$. Keeping the cell in this condition, the alkyl halide is added and the current is monitored until $[\text{Cu}^{\text{I}}\text{L}^+]$ decreases to small values. Some experiments were performed by monitoring the rate of formation of $\text{XCu}^{\text{II}}\text{L}^+$. In this case the potential was stepped from $E_i \geq -0.20$ V to values well beyond the reduction potential of $\text{XCu}^{\text{II}}\text{L}^+$ (see Figs. S2 and S3). In all cases these two approaches gave practically the same results.

The limiting current, I_L , for the oxidation of $\text{Cu}^{\text{I}}\text{L}^+$ is correlated to the bulk concentration, $[\text{Cu}^{\text{I}}\text{L}^+]^*$, of the metal complex thorough the Levich equation:⁵

$$I_L = 0.62nFAD^{2/3}\omega^{1/2}\nu^{-1/6}[\text{Cu}^{\text{I}}\text{L}^+]^* \quad (\text{S1})$$

where F is the Faraday constant, D is the diffusion coefficient of the electroactive species, ω is the angular velocity of rotating disc electrode, A is the area of the electrode and ν is the kinetic viscosity.

For relatively slow reactions, the activation kinetics can be examined under pseudo-first-order conditions, that is, using $[\text{RX}]_0/[\text{Cu}^{\text{I}}\text{L}^+]_0 \geq 20$. The reaction rate can be expressed as the rate of disappearance of $\text{Cu}^{\text{I}}\text{L}^+$:

$$-\frac{d[\text{Cu}^{\text{I}}\text{L}^+]}{dt} = k_{\text{act}}[\text{Cu}^{\text{I}}\text{L}^+][\text{RX}] = k'[\text{Cu}^{\text{I}}\text{L}^+] \quad (\text{S2})$$

$$\ln[\text{Cu}^{\text{I}}\text{L}^+] = \ln[\text{Cu}^{\text{I}}\text{L}^+]_0 - k't \quad (\text{S3})$$

where $[\text{Cu}^{\text{I}}\text{L}^+]_0$ is the initial concentration of $\text{Cu}^{\text{I}}\text{L}^+$ and $k' = k_{\text{act}}[\text{RX}]_0$. Substituting $[\text{Cu}^{\text{I}}\text{L}^+]$ and $[\text{Cu}^{\text{I}}\text{L}^+]_0$ in eq. (S3) from eq. (S1) gives

$$\ln I_L = \ln I_L^0 - k't \quad (\text{S4})$$

This approach was used in the case benzyl chloride. Reactions between $\text{Cu}^{\text{I}}\text{L}^+$ and RX were carried out at different RX concentrations to obtain a series of k' values as a function of $[\text{RX}]$. A plot of k' vs $[\text{RX}]$ shows a straight line with a slope corresponding to k_{act} (Fig. S5).

For fast reactions, second-order conditions were chosen. If the reaction is performed using

$[\text{Cu}^{\text{I}}\text{L}^+]_0 = [\text{RX}]_0$, the kinetic rate law becomes:

$$-\frac{d[\text{Cu}^{\text{I}}\text{L}^+]}{dt} = k_{\text{act}}[\text{Cu}^{\text{I}}\text{L}^+][\text{RX}] = k_{\text{act}}[\text{Cu}^{\text{I}}\text{L}^+]^2 \quad (\text{S5})$$

$$\frac{1}{[\text{Cu}^{\text{I}}\text{L}^+]} - \frac{1}{[\text{Cu}^{\text{I}}\text{L}^+]_0} = k_{\text{act}}t \quad (\text{S6})$$

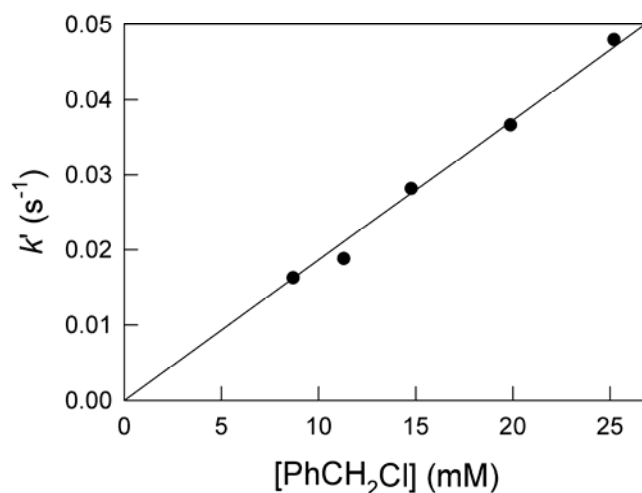


Figure S5. Observed activation rate constant k' as a function of initiator concentration for the reaction between $\text{Cu}^{\text{I}}\text{L}^+$ and PhCH_2Cl , in $\text{MeCN} + 0.1 \text{ M Et}_4\text{NBF}_4$ at 25°C .

The concentration of $\text{Cu}^{\text{I}}\text{L}^+$ can be calculated from the limiting current according to eq. (S1). Since during the experiment all parameters of eq. (S1) remain constant except I_L and $[\text{Cu}^{\text{I}}\text{L}^+]$, the relation between these two parameters can be expressed as follows

$$[\text{Cu}^{\text{I}}\text{L}^+] = \frac{I_L}{0.62nFAD^{2/3}\omega^{1/2}v^{-1/6}} = \frac{I_L}{I_L^0}[\text{Cu}^{\text{I}}\text{L}^+]_0 \quad (\text{S7})$$

At least three independent experiments were carried out for each alkyl halide, which gave similar k_{act} values, which were used to calculate the average values reported in the paper.

Some examples of chronoamperometry and kinetic analysis are reported in Figures S6 and S7.

5. Determination of activation rate constants in the presence of halide ions

When the system contains halide ions, different Cu^{I} complexes are formed, with a distribution depending the concentration of X^- . These Cu^{I} species give rise to a complicated voltammetric

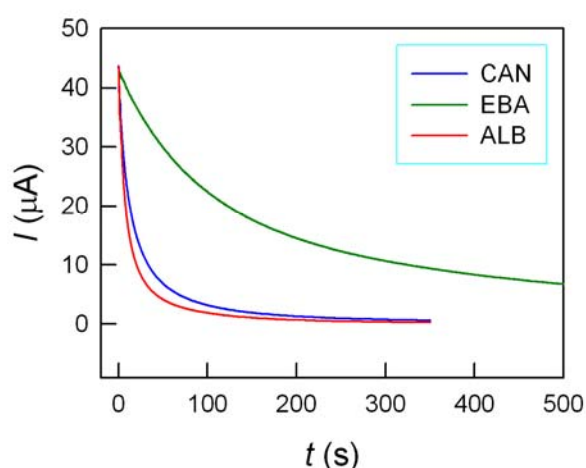


Figure S6. Chronoamperometry of 0.50 mM $[\text{Cu}^{\text{I}}(\text{MeCN})_4]\text{BF}_4$ + 0.50 mM Me_6TREN + 0.50 mM RX + 10 mM TEMPO, recorded at RDE ($\omega = 2500$ rpm) in MeCN + 0.1 M Et_4NBF_4 at 25 °C. Single step potential from -0.3 V to 0.1 V vs SCE.

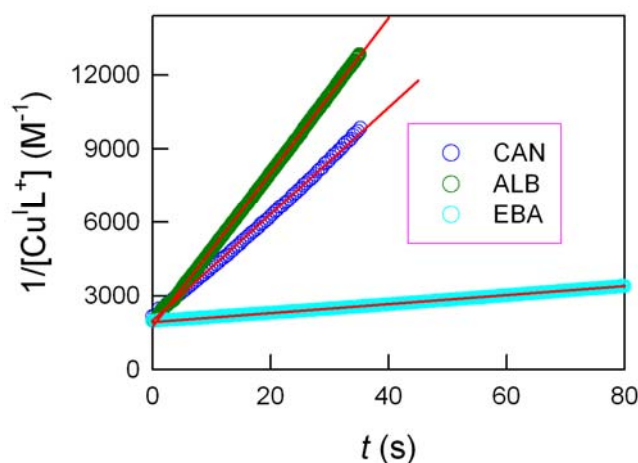


Figure S7. Kinetic analysis of the reaction between $\text{Cu}^{\text{I}}\text{L}^+$ and RX according to eq. S6. Reaction conditions: 0.50 mM $[\text{Cu}^{\text{I}}(\text{MeCN})_4]\text{BF}_4$ + 0.50 mM Me_6TREN + 0.50 mM RX + 10 mM TEMPO in MeCN + 0.1 M Et_4NBF_4 at 25 °C.

pattern, which is not suitable for the monitoring of the reaction kinetics. In contrast, Cu^{II} gives essentially $\text{XCu}^{\text{II}}\text{L}^+$ even in the presence of excess X^- with respect Cu^{II} and L. This system shows a single cathodic wave due to the reduction of $\text{XCu}^{\text{II}}\text{L}^+$ to $\text{XCu}^{\text{I}}\text{L}$. We used this wave to monitor the reaction kinetics in the presence of X^- . Chronoamperometric experiments were performed as described in section 4 by stepping the potential from an initial value $E_i \geq -0.20$ V vs SCE to a final value $E_f \leq -0.65$ V vs SCE for $\text{X} = \text{Cl}^-$ and $E_f \leq -0.50$ V vs SCE for $\text{X} = \text{Br}^-$. In this case, the rate of the reaction is given by

$$\frac{d[\text{XCu}^{\text{II}}\text{L}^+]}{dt} = k_{\text{act}}[\text{Cu}^{\text{I}}\text{L}^+][\text{RX}] = k_{\text{act}}([\text{Cu}^{\text{I}}\text{L}^+]_0 - [\text{XCu}^{\text{II}}\text{L}^+])[\text{RX}] \quad (\text{S8})$$

where $[\text{Cu}^{\text{I}}\text{L}^+]_0$ is the initial concentration of Cu^{I} . Resolving this differential equation under pseudo-first-order ($[\text{RX}]_0 \gg [\text{Cu}^{\text{I}}\text{L}^+]_0$) or second-order conditions with $[\text{Cu}^{\text{I}}\text{L}^+]_0 = [\text{RX}]_0$ gives eqs (S9) and (S10), respectively.

$$\ln([\text{Cu}^{\text{I}}\text{L}^+]_0 - [\text{XCu}^{\text{II}}\text{L}^+]) = \ln[\text{Cu}^{\text{I}}\text{L}^+]_0 - k't \quad (\text{S9})$$

$$\frac{1}{[\text{Cu}^{\text{I}}\text{L}^+]_0 - [\text{XCu}^{\text{II}}\text{L}^+]} - \frac{1}{[\text{Cu}^{\text{I}}\text{L}^+]_0} = k_{\text{act}}t \quad (\text{S10})$$

The rate constants obtained for each RX at different X^- concentrations are listed in Table S1.

Table S1. Observed rate constants of activation of RX by $\text{Cu}^{\text{I}}\text{L}^+$ in MeCN + 0.1 M Et_4NBF_4 .^a

RX	$[\text{X}^-]^b$ mM	k_{obs} $\text{M}^{-1}\text{s}^{-1}$
Benzyl chloride ^c	0	1.86
	0.56	1.39
	1.07	0.78
	2.94	0.31
	5.75	0.14
Chloroacetonitrile	0	230
	0.51	142
	1.05	111
	3.0	58.5
	5.69	15.2
Ethyl bromoacetate	0	22.0
	0.50	19.2
	1.02	18.4
	2.43	16.1
	5.22	12.4
Allyl bromide	0	326
	0.50	291
	1.0	274
	2.57	230
	5.15	175

^aUnless otherwise stated, the general reaction conditions were: $[\text{Cu}^{\text{I}}\text{Me}_6\text{TREN}^+]_0 = [\text{RX}]_0 = 5 \times 10^{-4}$ M; $[\text{TEMPO}] = 5 \times 10^{-3}$ M; $T = 25$ °C. ^b $\text{X}^- = \text{Cl}^-$ or Br^- , depending on the type of RX. ^cInvestigated under pseudo-first-order conditions ($[\text{RX}]/[\text{Cu}^{\text{I}}\text{L}^+] \geq 20$).

References

- 1 J. Queffelec, S. G. Gaynor and K. Matyjaszewski, *Macromolecules*, 2000, **33**, 8629.
- 2 A. A. Isse, G. Sandonà, C. Durante and A. Gennaro, *Electrochim. Acta*, 2009, **54**, 3235.
- 3 L. Alderighi, P. Gans, A. Ienco, D. Peters, A. Sabatini and A. Vacca, *Coord. Chem Rev.*, 1999, **184**, 311.
- 4 N. Bortolamei, A. A. Isse, V. B. Di Marco, A. Gennaro and K. Matyjaszewski, *Macromolecules*, 2010, **42**, 6050.
- 5 A. J. Bard and L. R. Faulkner, *Electrochemical Methods*, 2nd ed.; John Wiley & Sons: New York, 2001.